Cation-Dependent Role of Water on the Dynamics and Ionic Conductivity of Levulinate Based Ionic Liquids

Georgios Tsonos , Sotiria Kripotou , Georgios Mavroeidis , Christos Tsonos * , Lorenzo Guazzelli , Luca Guglielmero , Ilias Stavrakas , Kostas Moutzouris

Posted Date: 5 March 2026

doi: 10.20944/preprints202603.0452.v1

Keywords: ionic liquids; levulinate-based ionic liquids; water–ionic liquid interactions; broadband dielectric spectroscopy; ionic conductivity; charge transport; conductivity relaxation; cation structure

 doi:10.20944/preprints202603.0452.v1

Article

Cation-Dependent Role of Water on the Dynamics and Ionic Conductivity of Levulinate Based Ionic Liquids

Georgios Tsonos [1], Sotiria Kripotou [1], Georgios Mavroeidis [1], Christos Tsonos [2,*], Lorenzo Guazzelli [3], Luca Guglielmero [3], Ilias Stavrakas [1] and Kostas Moutzouris [1]

[1] Department of Electrical and Electronics Engineering, University of West Attica, 12244 Athens, Greece

[2] Department of Physics, University of Thessaly, 35100 Lamia, Greece

[3] Department of Pharmacy, University of Pisa, Via Bonanno 6, 56126 Pisa, Italy

* Correspondence: christostsonos@uth.gr

Abstract

The effect of water on the dynamics and ionic conductivity of the ionic liquids 1-ethyl-1-methylpyrrolidinium levulinate ([C_2C_1Pyr]Lev) and 1-butyl-1- methylpyrrolidinium levulinate ([C_4C_1Pyr]Lev) was investigated using differential scanning calorimetry (DSC) and broadband dielectric spectroscopy (BDS) over a wide temperature range. Although both ILs share the same levulinate anion, water induces markedly different dynamical responses depending on cation structure. In both systems, water acts as a plasticizer, lowering the glass transition temperature; however, the extent of plasticization and the resulting relaxation dynamics are cation-dependent. Stronger water–cation interactions are observed in [C_2C_1Pyr]Lev, whereas in [C_4C_1Pyr]Lev, water primarily disrupts alkyl-chain packing, enhancing ionic mobility. Increasing hydration shifts the main relaxation to higher frequencies and increases liquid fragility, while translational ionic motion remains partially decoupled from structural relaxation. These results demonstrate that water plays a cation-specific and mechanistically distinct role in levulinate-based ILs, providing new insights into hydration-controlled glassy dynamics and charge transport relevant for the design of IL-based electrolytes under non-anhydrous conditions.

Keywords: ionic liquids; levulinate-based ionic liquids; water–ionic liquid interactions; broadband dielectric spectroscopy; ionic conductivity; charge transport; conductivity relaxation; cation structure

1. Introduction

Ionic liquids (ILs) are salts composed entirely of ions, characterized by negligible vapor pressure, wide electrochemical windows, and high thermal and chemical stability [1]. These properties, combined with the ability to tailor cation and anion structures, make ILs attractive for diverse applications [2], particularly in energy-related devices where they function as electrolytes in batteries, supercapacitors, and other electrochemical systems [3–10]. Structural tunability allows rational design of ILs with optimized macroscopic properties for specific technological needs.

A critical factor affecting IL performance is water, which is often present due to the hygroscopic nature of most ILs [11–13]. Even small amounts of water can significantly influence viscosity, glass transition temperature (Tg) and ionic conductivity [14–26]. Water can act as a plasticizer, lowering Tg and enhancing ionic mobility, but the microscopic effects depend on its organization within the ionic matrix, including ion hydration, cluster formation, or partitioning into polar and nonpolar domains [23,25,27]. This complex interplay often leads to system-dependent behavior, including acceleration of ionic motion or partial decoupling of translational ionic motion from structural relaxation.

 doi:10.20944/preprints202603.0452.v1

In this study, we investigate the impact of absorbed moisture on Tg, ionic conductivity, and molecular dynamics in two levulinate based ILs: 1-ethyl-1-methylpyrrolidinium levulinate and 1-butyl-1-methylpyrrolidinium levulinate. Because the cations differ only in the length of the alkyl chain attached to the pyrrolidinium nitrogen, while anion remains the same, we can directly assess how this variation influences water-ion interactions and structural organization within the ionic matrix. By combining differential scanning calorimetry (DSC) with broadband dielectric spectroscopy (BDS), we aim to establish clear correlations between cation structure, water-induced plasticization, and ionic mobility, providing insight into the molecular mechanisms governing hydrated ILs and informing the design of IL-based electrolytes for energy applications.

2. Materials and Methods

2.1. Materials and Sample Preparation

The ionic liquids studied are 1-ethyl-1-methylpyrrolidinium levulinate, [C2C1Pyr]Lev, and 1-butyl-1-methylpyrrolidinium levulinate, [C4C1Pyr]Lev. These ionic liquids share a common levulinate (Lev) anion, while their cations differ in the length of the alkyl chain attached to the nitrogen atom of the pyrrolidinium ring. The chain consists of two carbons (C2C1Pyr) in the first case and four carbons (C4C1Pyr) in the second. The preparation of the materials is described in [28].

Two sets of samples were prepared: those maintained in a desiccator over P2O5 for an extended period, and those exposed to ambient conditions (temperature 25-30 °C and relative humidity 50-60%) for five days. The water content of each sample was determined by weighing the sample before and after the differential scanning calorimetry measurements, during which water evaporation was observed. The water percentages reported hereafter refer to the water content relative to the dry mass and were calculated using the following equation

$$h_w = \frac{m_h - m_d}{m_d} 100$$

where mh is the mass of the sample before water evaporation and md is the mass of the sample after. Hereafter, the samples will be referred to as hw%, where hw represents the water percentage by weight. For the ionic liquid [C2C1Pyr]Lev, samples with water concentrations of 9% and 59% were prepared, while for [C4C1Pyr]Lev, samples with water concentrations of 10% and 44% were prepared.

2.2. Differential Scanning Calorimetry (DSC)

Differential Scanning Calorimetry (DSC) measurements were conducted using a TA Q200 instrument (TA Instruments). The samples were placed in aluminum pans and sealed with a crimp press. The mass of both the samples and the pans was measured using a high-precision balance. Subsequently, the pans were pierced to allow for water evaporation and placed into the calorimeter. The experimental protocol involved cooling the sample from ambient temperature down to -150 °C at a rate of -10 °C/min, followed by an isothermal hold for 2 minutes, and then heating the sample up to 200 °C at a rate of 10 °C/min.

2.3. Broadband Dielectric Spectroscopy (BDS)

Dielectric measurements were performed using an experimental setup consisting of an Alpha-Analyzer frequency response analyzer and a Novocool temperature control system (Novocontrol Technologies). The samples were placed in a liquid dielectric cell, consisting of a Teflon cylinder with metal electrodes at the top and bottom. The cell had a thickness of 2 mm and an electrode diameter of 11 mm. An alternating voltage of 1 Vrms was applied across the electrodes. Isothermal measurements were carried out in the frequency range of 0.1 Hz to 1 MHz and over a temperature range of -100 °C to 60 °C, with a temperature step of 10 °C.

3. Results and Discussion

 doi:10.20944/preprints202603.0452.v1

3.1. DSC Results

Figure 1 presents the DSC thermograms of [C2C1Pyr]Lev and [C4C1Pyr]Lev at different hydration levels. Upon heating, all samples exhibit a step-like change in the heat flow in the low temperature region (-100 to -50 °C), attributed to the glass transition. At higher temperatures (around 100 °C), a pronounced endothermic peak corresponding to water evaporation is observed. In both ionic liquids, increasing water content shifts the glass transition to lower temperatures, indicating a clear plasticizing effect of water. Simultaneously, the evaporation peak shifts to lower temperatures and increases in magnitude with increasing hydration, reflecting the higher amount of absorbed water and its modified thermal stability within the ionic matrix.

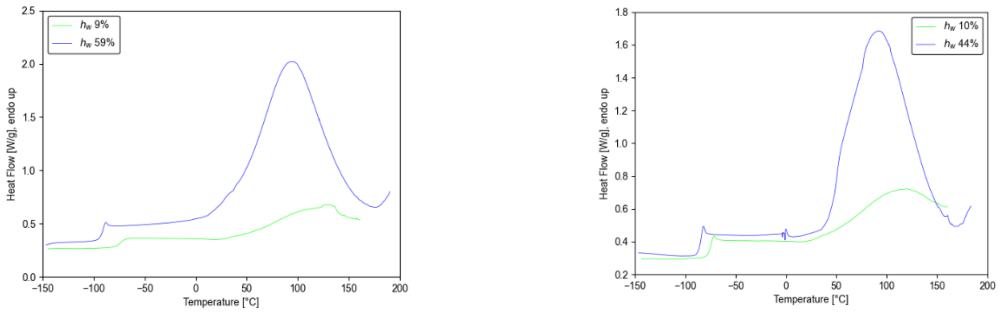

Figure 1. DSC thermograms for the ionic liquids [C2C1Pyr]Lev (left) and [C4C1Pyr]Lev (right).

Table 1 summarizes the glass transition temperature (Tg), the heat capacity change at Tg (ΔCp), the enthalpy of water evaporation (ΔH), and the peak evaporation temperature (Tmax). For [C2C1Pyr]Lev, Tg decreases from -73 °C to -92 °C as the water content increases from 9 wt% to 59 wt% confirming the pronounced plasticizing effect of water. A corresponding increase in ΔCp is observed, consistent with enhanced molecular mobility and increased configurational freedom in the hydrated samples. ΔH increases with water content, reflecting the larger amount of absorbed water, while Tmax decreases from 130 °C to 95 °C. The reduction in Tmax suggests stronger water–ionic liquid interactions at lower hydration levels and progressively weaker binding as the water content increases.

A similar trend is observed for [C4C1Pyr]Lev, where Tg decreases from -76 °C to -85 °C as the water content increases from 10 wt% to 44 wt%. The corresponding decrease in Tmax from 119 °C to 92 °C again indicates a weakening of specific water-ionic liquid interactions at higher hydration levels. Notably, the magnitude of Tg depression is smaller, and the Tmax of the dry sample is lower compared to [C_2C_1Pyr]Lev, suggesting differences in the manner by which water interacts with the cation structure and modifies the local organization of the ionic matrix.

Table 1. Thermal results of DSC measurements of hydrated ionic liquids.

IL	h_w (%)	T_g (°C)	ΔC_p (J/g °C)	ΔH (J/g)	T_{max} (°C)
[C2C1Pyr]Lev	9	-73	0.53	67	130
[C2C1Pyr]Lev	59	-92	0.85	600	95
[C4C1Pyr]Lev	10	-76	0.71	72	119
[C4C1Pyr]Lev	44	-85	0.85	488	92

It should be noted here that a previous study on [C4C1Pyr]Lev reported melting and crystallization at 41.6 °C and -33.3 °C, respectively, with a glass transition observed only during the first heating cycle and disappearing after dehydration at elevated temperatures [28]. In contrast, the hydrated samples investigated in the present work exhibit exclusively glass transitions, with no

 doi:10.20944/preprints202603.0452.v1

evidence of crystallization. This behavior suggests that the presence of sufficient water suppresses crystallization, likely by disrupting the regular packing of ions and modifying intermolecular interactions within the ionic matrix.

For both ionic liquids investigated, water acts as a plasticizer, progressively lowering the glass transition temperature. Such Tg depression upon hydration has been widely reported for ionic liquids and is generally associated with reduced viscosity and weakened ion–ion interactions [25,26,29–31], although opposite trends can occur in systems with less hydrophilic anions [32]. DSC measurements reveal that the structure of the cation strongly influences the degree of plasticization, with Tg depression being more pronounced for [C_2C_1Pyr]Lev than for [C_4C_1Pyr]Lev. The heat capacity change at Tg (ΔCp) increases with rising water content in both ILs, showing no significant cation dependence. In contrast, the peak evaporation temperature (Tmax) is consistently lower for [C_4C_1Pyr]Lev than for [C_2C_1Pyr]Lev across all hydration levels, indicating stronger water–ionic liquid interactions in [C_2C_1Pyr]Lev. Spectroscopic evidence further indicates that water induces microstructural heterogeneity rather than acting as a simple diluent, and that alkyl-chain length modulates water accommodation, influencing both polar and nonpolar domains [29,33]. In line with these observations, the stronger Tg depression in [C_2C_1Pyr]Lev likely arises from direct water–cation interactions, whereas in [C_4C_1Pyr]Lev, water primarily perturbs alkyl-chain packing. Overall, the combined effect of network softening and hydration-induced structural reorganization underlies the observed cation-dependent thermal behavior of these levulinate-based ionic liquids.

3.2. DRS Results

3.2.1. Dielectric Spectra

Figure 2 presents representative dielectric spectra for [C_2C_1Pyr]Lev at 59% water content over the temperature range from -100 to -30 °C. Panels (a–e) show the real (ε′) and imaginary (ε″) parts of the dielectric function, the derivative of the real part (εderiv″, free from DC conductivity contributions [34], the real conductivity (σ′), and the imaginary part of the electric modulus (M″), all plotted as a function of frequency.

At -100 °C, a temperature below Tg, two peaks are observed in the imaginary part of the dielectric function ε″ (Figure 2b), indicated by arrows on the corresponding plot.

 doi:10.20944/preprints202603.0452.v1

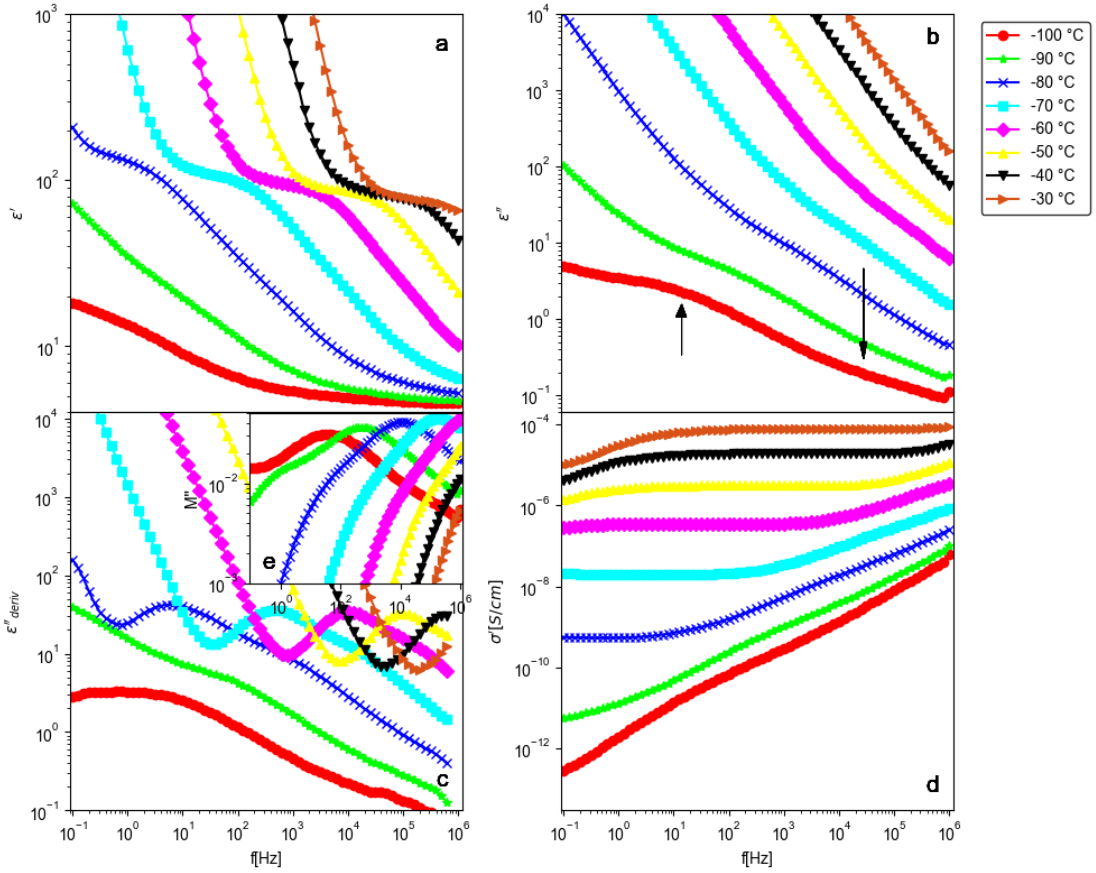

Figure 2. Dielectric measurement plots for the [C2C1Pyr]Lev ionic liquid with a water content of 59%, over a temperature range from -100 to -30 °C. The real part of the dielectric function ε′ (a), the imaginary part of the dielectric function ε″ (b), the derivative of the real part of the dielectric function, ε_{deriv}″ (c), the real part of complex conductivity σ′ (d) and the imaginary part of the electric modulus M″ (e) are shown as a function of frequency f.

These peaks correspond to two secondary dielectric relaxation processes. The contribution of each mechanism is manifested as a step-like change in the real part of the dielectric function ε′ (Figure 2a), and as a shoulder or peak in the plots of the derivative εderiv″ (Figure 2c) and the imaginary part of the electric modulus M″ (Figure 2e). As the temperature increases, these mechanisms shift toward higher frequencies. The faster process, also visible in the dry sample, is attributed to localized ion motions, consistent with previous reports in the literature [35,36], whereas the slower process appears only in the hydrated sample and is associated with water. A detailed analysis of these secondary relaxations, however, lies beyond the scope of the present study. As the temperature increases above Tg (>-90 °C), a strong increase in σ′ (Figure 2d) is observed at low frequencies, forming a nearly frequency-independent plateau that grows with temperature. Simultaneously, a pronounced step in ε′, a peak in ε″deriv, and a shoulder in M″ appear in the same frequency range, also shifting to higher frequencies with temperature. This process corresponds to the main relaxation (*α*-relaxation or conductivity relaxation), associated with the motion of ions. In ε″, the *α*-relaxation is masked at low frequencies by the linear increase due to DC conductivity. At frequencies lower than those of the main relaxation deviations in ε′, εderiv″, and σ′ are attributed to electrode polarization [37].

At higher temperatures (not shown), the dielectric spectra become increasingly dominated by DC conductivity and electrode polarization. A similar pattern is observed for hydrated [C_4C_1Pyr]Lev, with secondary relaxations below Tg (with the exception that only a single process is detected at the lowest water content) and a dominant *α*-relaxation above Tg, although the characteristics of these processes differ from those of [C_2C_1Pyr]Lev, indicating that the underlying ionic dynamics and charge transport mechanisms are preserved across both systems.

 doi:10.20944/preprints202603.0452.v1

3.2.2. Temperature - Water Dependence of Dynamics and Conductivity

The main focus of the present work is the investigation of the effect of water on the DC conductivity and the primary α-relaxation of [C_2C_1Pyr]Lev and [C_4C_1Pyr]Lev ionic liquids. To extract the peak frequencies and relaxation strengths of the α-relaxation, fitting procedures were applied to the ε'' vs. frequency plots in selected regions around the ε''deriv peaks. For this purpose, the following equation was used to model the data:

$$\varepsilon'' = Af^{-1} + \mathrm{Im}\left[\varepsilon_\infty + \frac{\Delta\varepsilon}{(1+(j\omega\tau)^\alpha)^\beta}\right] \quad (1)$$

The first term of equation (1), where A is a constant, accounts for the contribution of DC conductivity to ε'', while the second term corresponds to the imaginary part of the Havriliak–Negami equation [38] and describes the contribution of the main α-relaxation. $\Delta\varepsilon$ is the dielectric strength (dielectric increment) of the main relaxation, ε_∞ is the dielectric constant at the high-frequency limit, τ is a characteristic relaxation time related to the peak frequency (f_m) of ε'', and α, β are shape parameters with values in the range 0-1.

Figure 3 presents the Arrhenius plots of the main relaxation, illustrating its temperature dependence for the ionic liquids [C_2C_1Pyr]Lev and [C_4C_1Pyr]Lev. The frequencies (f_m) of the ε'' peaks at various temperatures, obtained from the best fit of equation (1), were used to construct the plots. As shown in Figure 3, the main relaxation of [C_2C_1Pyr]Lev samples with 9% and 59% water content, as well as [C_4C_1Pyr]Lev with 44% water content, follows Vogel–Fulcher–Tammann (VFT) behavior [39–41]. An exception is observed for [C_4C_1Pyr]Lev with 10% water content, which exhibits Arrhenius-type behavior.

For both ionic liquids at different hydration levels, the main relaxation shifts to higher frequencies at a given temperature as the water content increases across the entire temperature range. This plasticizing effect of water on the main relaxation is likely related to changes in the viscosity of the samples. According to the Debye–Stokes–Einstein relation, the rotational relaxation time of a particle in a liquid medium is directly proportional to viscosity. Although deviations from this relationship have been reported in ionic liquids [42], it has been shown to hold approximately in similar systems [43,44]. Therefore, the observed increase in the peak frequency f_m of the main relaxation with increasing water content may be attributed to the corresponding decrease in viscosity.

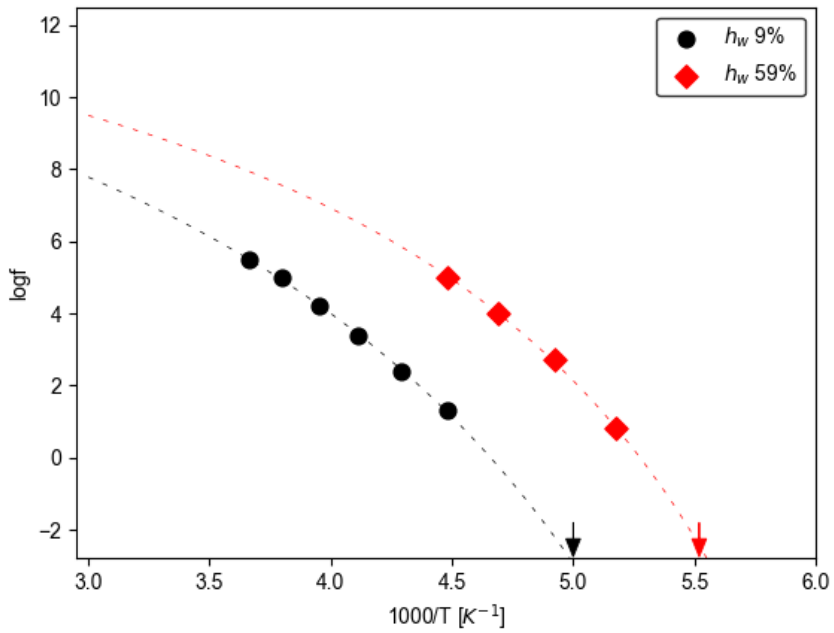

 doi:10.20944/preprints202603.0452.v1

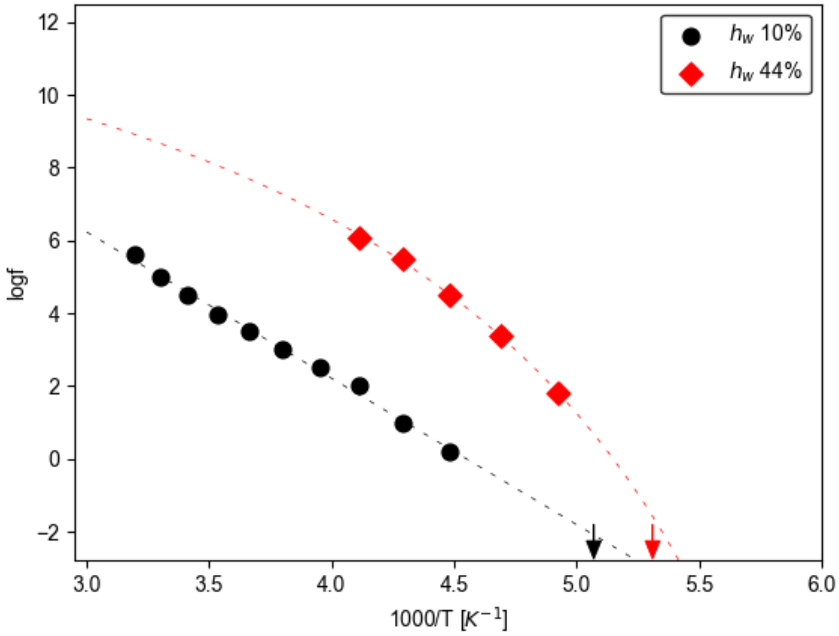

Figure 3. Arrhenius plots of the main α-relaxation, illustrating its temperature dependence for the ionic liquids [C2C1Pyr]Lev (upper panel) and [C4C1Pyr]Lev (lower panel). Arrows indicate the Tg values determined from DSC measurements.

For the ionic liquid samples exhibiting VFT behavior (Figures 3), the best fit to the experimental results was performed using the empirical equation:

$$f_m = f_o e^{-\frac{DT_o}{T-T_o}} \quad (2)$$

which often describes the non-Arrhenius temperature dependence dynamics of glassy systems. In Equation (2), To is the Vogel temperature, typically located a few tens of Kelvin below the material's glass transition temperature. fo is the pre-exponential factor, which corresponds to an inverse attempt frequency, and D is the so-called strength parameter [45]. Parameter D is used to distinguish between strong and fragile glass formers and serves as a measure of the deviation from Arrhenius behavior. Alternatively, the fragility index m is also used for the classification of glass formers. Both parameters are connected via the relation m=16+590/D [46]. Higher values of m (lower values of D) correspond to more fragile temperature characteristics and stronger deviations from Arrhenius behavior. The fits in Figures 3 are extrapolated to $\log f_m = -2.79$, which corresponds to the characteristic time τ=100 s. The temperature at which the relaxation time of the main α-relaxation reaches 100 s is commonly defined as the dielectric glass transition temperature (T_{gdiel}) [47].

As shown in Figure 3, the Tgdiel values for the [C2C1Pyr]Lev samples are nearly identical, whereas those for [C4C1Pyr]Lev are slightly higher (by approximately 3–4 K). This indicates that, in [C2C1Pyr]Lev, the mobility of the ions involved in the main relaxation closely follows the mobility of the bulk ionic liquid. In contrast, the small shift observed for [C4C1Pyr]Lev points to a slight decoupling between ionic motion and structural relaxation. Consequently, the observed increase in ion mobility with increasing hydration is primarily attributed to the corresponding decrease in T_g. Moreover, for [C4C1Pyr]Lev, increasing the water content from 10% to 44% has a more pronounced effect on the shift of the main relaxation frequency f_m than the corresponding shift observed for [C2C1Pyr]Lev. This behavior is consistent with the stronger influence of water on the T_g of [C4C1Pyr]Lev.

For the [C4C1Pyr]Lev sample with 10% water content, the experimental data were best described using the Arrhenius equation:

 doi:10.20944/preprints202603.0452.v1

$$f_m = f_o e^{-\frac{E}{kT}} \quad (3)$$

where f_o is a pre-exponential factor and E is the activation energy.

Table 2 summarizes the parameters obtained from fitting Equation (2) to the experimental data. The Vogel temperature, T_0, falls within a narrow range of 135–140 K for all three samples: 9% and 59% water content in [C_2C_1Pyr]Lev, and 44% water content in [C_4C_1Pyr]Lev. The lowest fragility index, m = 49, is observed for the sample with the lowest water content (9% [C_2C_1Pyr]Lev). In contrast, the two samples with higher water contents exhibit larger and nearly identical fragility indices (m = 66 and 67), indicating a stronger deviation from Arrhenius behavior. For the [C_4C_1Pyr]Lev sample containing 10 wt% water, the activation energy associated with the main relaxation process was determined using Equation (3), yielding a value of E = 0.80 eV.

Table 2. Parameter values from the VTF equation fits for main relaxation and dc conductivity.

	Main relaxation				DC conductivity			
IL	B	D	T_o (K)	m	B	D	T_o (K)	m
[C2C1Pyr]Lev 9%	2384	17.7	135	49	1796	12.3	146	64
[C2C1Pyr]Le559 %	1593	11.7	136	66	1217	8.5	143	85
[C4C1Pyr]Lev 44%	1630	11.7	140	67	1239	8.4	147	86

Figure 4 presents the dielectric relaxation strength, Δε, of the main relaxation as a function of temperature for the [C_2C_1Pyr]Lev and [C_4C_1Pyr]Lev samples at different hydration levels. For the [C_2C_1Pyr]Lev samples, Δε decreases with increasing temperature. In contrast, the [C_4C_1Pyr]Lev sample containing 10 wt% water exhibits an increase in Δε with rising temperature. Moreover, the absolute values of Δε in this sample are significantly higher than those of the 44 wt% [C_4C_1Pyr]Lev sample, where Δε decreases with temperature, following the same trend observed for the [C_2C_1Pyr]Lev systems. It should be noted that the dielectric relaxation strength, Δε, is related to the number density of mobile ions and therefore provides insight into changes in ionic mobility and charge carrier concentration [48].

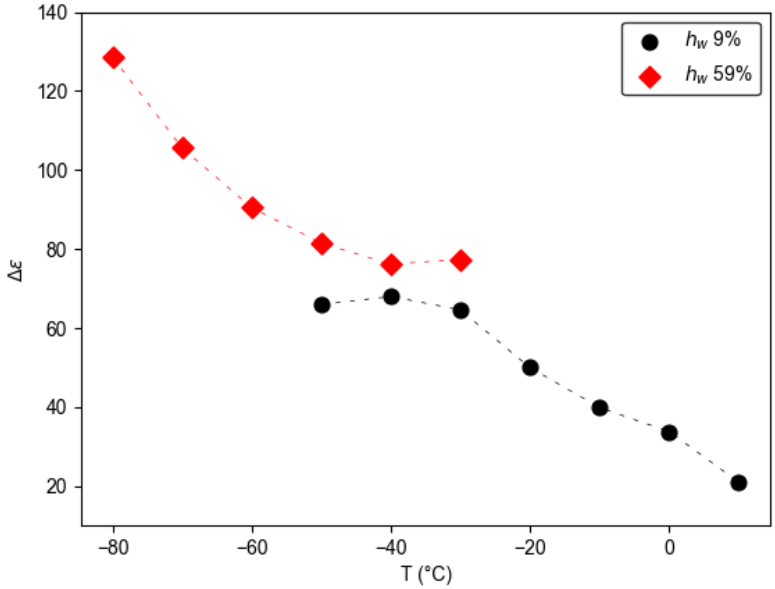

 doi:10.20944/preprints202603.0452.v1

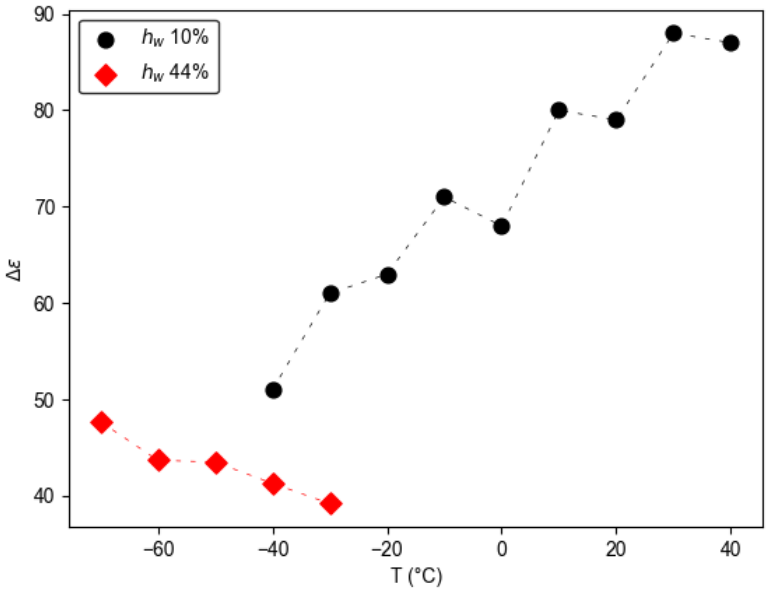

Figure 4. Dielectric relaxation strength, Δε, of the main relaxation as a function of temperature for the [C2C1Pyr]Lev (upper panel) and [C4C1Pyr]Lev (lower panel) samples.

Figure 5 shows the Arrhenius representations of the dc conductivity, highlighting its temperature dependence for the [C_2C_1Pyr]Lev and [C_4C_1Pyr]Lev ionic liquids. The dc conductivity values, σ_{dc}, were extracted from the frequency-independent plateaus observed at each temperature.With the exception of the 10 wt% [C_4C_1Pyr]Lev sample, which follows Arrhenius behavior, the remaining three ionic liquid samples exhibit a non-Arrhenius temperature dependence that is well described by the empirical Vogel–Fulcher–Tammann (VFT) equation:

$$\sigma_{dc} = \sigma_o e^{-\frac{DT_o}{T-T_o}} \quad (4)$$

Figure 5 includes the corresponding fits of Equation (4) for the three samples displaying VFT behavior, while for the 10 wt% [C_4C_1Pyr]Lev sample, the best fit using the Arrhenius expression $\sigma_{dc} = \sigma_o \exp\left(-\frac{E}{kT}\right)$ is presented. The fits (shown in Figure 5) are extrapolated to $\sigma_{dc} \approx 10^{-15}$ S/cm. When ionic motion is coupled to the structural (α) relaxation, σ_{dc} is expected to approach this characteristic value at the glass transition temperature, Tg [49].

Table 2 summarizes the parameters obtained from fitting Equation (4) to the experimental data. The Vogel temperature, T_0, lies in the range 143–147 K for the three samples: 9% and 59% water content in [C_2C_1Pyr]Lev and 44% water content in [C_4C_1Pyr]Lev. The fragility indices (m) calculated from Equation (4) (Table 2) are higher for all ionic liquids than the corresponding m values derived from Equation (2) for the main relaxation dynamics. The lowest fragility index is observed for the sample with the lowest water content (9% [C_2C_1Pyr]Lev), with m = 64. The two samples with higher water contents exhibit larger and nearly identical fragility values (m = 85 and 86). For the 10 wt% [C_4C_1Pyr]Lev sample, the activation energy associated with dc conductivity, σ_{dc}, was determined to be E = 0.90 eV. In the hydrated ionic liquids examined in the present study, increasing water content results in higher fragility values. In contrast, the opposite trend has been reported for hydrated BMIMCl systems, where higher fragility values were observed at lower water contents [50]. This difference suggests distinct modes of water interaction and structural organization across different ionic liquid systems.

The ionic liquid samples [C_2C_1Pyr]Lev containing 9% and 59% water and [C_4C_1Pyr]Lev containing 10% and 44% water exhibit dc conductivity values at their respective glass transition temperatures of 0.8×10^{-13} S/cm, 2.4×10^{-13} S/cm, 1.8×10^{-13} S/cm, and 7.4×10^{-13} S/cm, respectively. These values, particularly for [C_4C_1Pyr]Lev with 59% water content. are significantly higher than the

 doi:10.20944/preprints202603.0452.v1

characteristic value of ~10^{-15} S/cm expected when ionic motion is fully coupled to structural relaxation. This finding indicates that although structural mobility is effectively frozen at T_g (as determined by DSC), a residual ionic mobility persists and continues to contribute to charge transport. Therefore, the translational ionic motion in the hydrated ionic liquids studied here appears to be partially decoupled from the structural relaxation process.

Similar decoupling behavior between ionic transport and structural (α) relaxation has been reported in several ionic liquid systems [42,51–53]. It should be noted, however, that in lidocaine-based ionic liquids no decoupling between ionic motion and structural relaxation was observed over a range of water contents [25]. These contrasting findings further emphasize that the interaction and structural organization of water within ionic liquids are highly system-dependent, leading to distinct coupling or decoupling behaviors between translational ionic motion and structural relaxation.

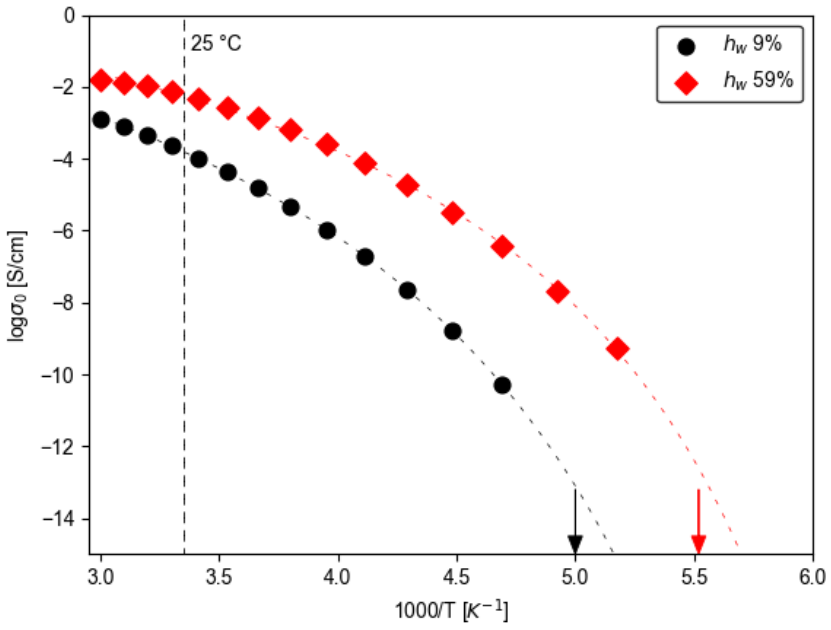

 doi:10.20944/preprints202603.0452.v1

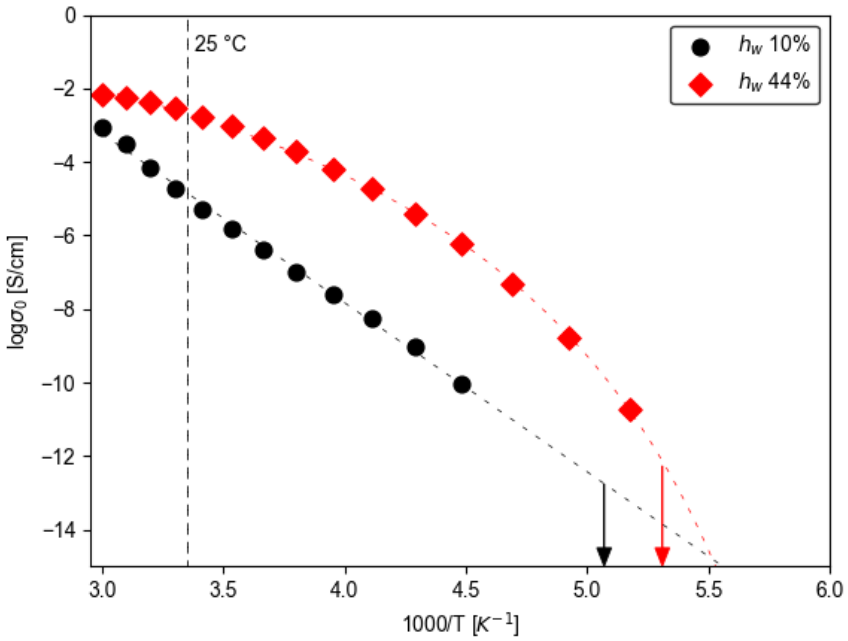

Figure 5. Arrhenius plots of dc conductivity, illustrating its temperature dependence for the [C2C1Pyr]Lev (upper panel) and [C4C1Pyr]Lev (lower panel) ionic liquids. The arrows show the Tg values from DSC measurements.

The dc conductivity at 25 °C, a key parameter for practical ionic liquid applications, increases with increasing water content in both ionic liquid systems. For the [C_2C_1Pyr]Lev ionic liquid, the conductivity rises by approximately one order of magnitude as the water content increases from 9% to 59%, reaching values on the order of 10^{-4} S/cm (9% sample) and 10^{-3} S/cm (59% sample). In the case of the [C_4C_1Pyr]Lev ionic liquid, the effect of water is even more pronounced. The 44% sample exhibits a conductivity at 25 °C of about 10^{-3} S/cm, nearly two orders of magnitude higher than that of the 10% sample (≈10^{-5} S/cm). Thus, the enhancement of conductivity induced by water is significantly stronger in [C_4C_1Pyr]Lev than in [C_2C_1Pyr]Lev. As discussed in [Sippel 2015] the conductivity at 25 °C is governed by both the glass transition temperature (Tg) and the fragility index (m). In agreement with this relationship, the 10% [C_4C_1Pyr]Lev sample—characterized by a relatively high T_g, Arrhenius-type temperature dependence, and consequently a low m value—exhibits the lowest dc conductivity at 25 °C. In contrast, the 59% [C_2C_1Pyr]Lev sample, which combines a lower T_g with a higher fragility index, shows the highest dc conductivity at the same temperature.

4. Conclusions

In the present work the effect of water on the dynamics and conductivity of [C2C1Pyr]Lev and [C4C1Pyr]Lev ionic liquids was investigated. It was found that the water content is a key factor controlling the dynamics and conductivity of ionic liquids, with effects that depend critically on the cation structure. The main results are summarized as follows:

Plasticizing Effect: For both ionic liquids, water acts as a plasticizer, effectively decreasing the glass transition temperature (Tg). The cation structure significantly influences the degree of Tg plasticization, which is more pronounced in the [C2C1Pyr] cation compared to [C4C1Pyr]. This suggests that the alkyl chain length of the cation plays a critical role in water organization and its interaction with the ionic liquid matrix.

Relaxation Dynamics: The temperature dynamics of the main relaxation and DC conductivity exhibit Vogel–Fulcher–Tammann (VFT) behavior in all samples, with the exception of the [C4C1Pyr]Lev sample with 10% water content, which follows Arrhenius behavior.

 doi:10.20944/preprints202603.0452.v1

Dielectric Strength: The dielectric strength (Δε) of the main relaxation decreases with increasing temperature for most samples. However, the [C4C1Pyr]Lev sample with 10% water content exhibits an increase in Δε with temperature.

Ion Mobility and Coupling: The mobility of ions participating in the main relaxation is consistent with the bulk mobility of the ionic liquid. At Tg, as extracted from DSC measurements, the DC conductivity values for all samples are noticeably higher than the expected value of 10^{-15} S/cm. This discrepancy indicates that while structural mobility is frozen at Tg, there is still notable ionic movement, proving that translational ionic motion in these hydrated systems is not well coupled to the structural relaxation measured by DSC.

Fragility Index: In all studied samples, higher water content leads to increased fragility index (m) values.

Conductivity at 25 °C: The DC conductivity at room temperature is determined by the synergy between Tg and the fragility index m. The 10% [C4C1Pyr]Lev sample (high Tg, Arrhenius behavior, lowest m) exhibits the lowest conductivity at 25 °C, whereas the 59% [C2C1Pyr]Lev sample (low Tg, high m) shows the highest conductivity.

In conclusion, water content is a critical parameter that drastically affects the dielectric and electrical properties of ionic liquids. The molecular structure of the ionic liquid components plays a decisive role in both the organization of water and the nature of the resulting interactions.

These results can be explained by the differing roles of water in the two ionic liquids. In [C_2C_1Pyr]Lev, water integrates into the ionic network, supporting structural integrity and enabling efficient ion transport. In [C_4C_1Pyr]Lev, water disrupts the packing of the long alkyl chains, reducing the number of ions actively participating in the main relaxation and partially decoupling ionic motion. This molecular-level distinction accounts for the observed differences in Δε, Tg, fragility, and conductivity, highlighting the crucial influence of cation architecture on hydration effects. These insights provide mechanistic guidance for the rational design of IL-based electrolytes under non-anhydrous conditions.

Author Contributions: Conceptualization and visualization were the responsibility of G.T., G.M., and S.K.; investigation and methodology were performed by G.T., G.M., S.K., Lo.G., Lu.G., I.S., K.M. and C.T.; validation and data analysis were performed by G.T., G.M., S.K.; writing and editing were performed by G.T. and S.K. All authors have read and agreed to the published version of the manuscript.

Institutional Review Board Statement: Not applicable.

Informed Consent Statement: Not applicable.

Data Availability Statement: Data are available upon reasonable request.

Conflicts of Interest: The authors declare no conflicts of interest.

References

1. Lei, Z.; Chen, B.; Koo, Y.-M., MacFarlane D.R. Introduction: Ionic Liquids. Chem. Rev. 2017, 117, 6633–6635.
2. Lei, Z.; Dai, C., Hallet, J, Shiflett M. Introduction: Ionic Liquids for Diverse Applications. Chem. Rev. 2024, 124, 7533–7535.
3. Watanabe M, Thomas ML, Zhang S, Ueno K, Yasuda T, Dokko K. Application of Ionic Liquids to Energy Storage and Conversion Materials. Electrochim. Acta 2017, 235, 633–642.
4. Tang, X.; Lv, S.; Jiang, K.; Zhou, G.; Liu, X. Recent Development of Ionic Liquid-Based Electrolytes in Lithium-Ion Batteries. J. Power Sources 2022, 542, 231792.
5. Matuszek, K.; Piper, S.L.; Brzeczek-Szafran, A.; Roy, B.; Saher, S.; Pringle, J. M.; MacFarlane, D. R. Unexpected Energy Applications of Ionic Liquids. Adv. Mater. 2024, 36, 2313023.
6. Noda, A.; Susan, M. A. B. H.; Kudo, K.; Mitsushima, S.; Hayamizu, K.; Watanabe, M. Brønsted Acid–Base Ionic Liquids as Proton-Conducting Nonaqueous Electrolytes. J. Phys. Chem. B 2003, 107, 4024–4033.

 doi:10.20944/preprints202603.0452.v1

7. Armand, M.; Endres, F.; MacFarlane, D.R.; Ohno, H.; Scrosati, B. Ionic-Liquid Materials for the Electrochemical Challenges of the Future. Nat. Mater. 2009, 8, 621–629.
8. MacFarlane, D.R.; Tachikawa, N.; Forsyth, M.; Pringle, J. M.; Howlett, P. C.; Elliott, G. D.; Davis, J. H.; Watanabe, M.; Simon, P.; Angell, C. A. Energy Applications of Ionic Liquids. Energy Environ. Sci. 2014, 7, 232–250.
9. Gao, X.; Wu, F.; Mariani, A.; Passerini, S. Concentrated Ionic-Liquid-Based Electrolytes for High-Voltage Lithium Batteries with Improved Performance at Room Temperature. ChemSusChem 2019, 12, 4185–4193.
10. Ma, X.; Yu, J.; Hu, Y.; Texter, J.; Yan, F. Ionic liquid/poly(ionic liquid)-based electrolytes for lithium batteries. Ind. Chem. Mater. 2023, 1, 39-59.
11. Cao, Y.; Chena, Y.; Sun, X.; Zhanga, Z.; Mu, T. Water sorption in ionic liquids: kinetics, mechanisms and hydrophilicity. Phys. Chem. Chem. Phys. 2012, 14, 12252–12262.
12. Di Francesco, F.; Calisi, N.; Creatini, M.; Melai, B.; Salvo, P.; Chiappe, C. Water sorption by anhydrous ionic liquids. Green Chem., 2011, 13, 1712-1717.
13. Freire, M.G.; Neves, C.M.S.S.; Marrucho, I.M.; Coutinho, J.A.P.; Fernandes, A.M. Hydrolysis of Tetrafluoroborate and Hexafluorophosphate Counterions in Imidazolium-Based Ionic Liquids. J. Phys. Chem. A 2010, 114, 3744–3749.
14. Ma, C.; Laaksonen, A.; Liu, C.; Lu, X.; Ji, X. The peculiar effect of water on ionic liquids and deep eutectic solvents. Chem. Soc. Rev. 2018, 47, 8685–8720.
15. Ausín, D.; Parajó, J.J.; Trenzado, J.L.; Varela, L.M.; Cabeza, O.; Segade, L. Influence of Small Quantities of Water on the Physical Properties of Alkylammonium Nitrate Ionic Liquids. Int. J. Mol. Sci. 2021, 22, 7334.
16. Rodriguez, H.; Brennecke, J.F. Temperature and composition dependence of the density and viscosity of binary mixtures of water plus ionic liquid. J. Chem. Eng. Data 2006, 51, 2145–2155.
17. Andanson, J.-M.; Meng, X.; Traïkia, M.; Husson, P. Quantification of the impact of water as an impurity on standard physico-chemical properties of ionic liquids. J. Chem. Thermodyn. 2016, 94, 169–176.
18. Grishina, E.P.; Ramenskaya, L.M.; Gruzdev, M.S.; Kraeva, O.V. Water effect on physicochemical properties of 1-butyl-3-methylimidazolium based ionic liquids with inorganic anions. J. Mol. Liq. 2013, 177, 267–272.
19. Widegren, J.A.; Laesecke, A.; Magee, J.W. The effect of dissolved water on the viscosities of hydrophobic room-temperature ionic liquids. Chem. Commun. 2005, 1610–1612.
20. Domańska, U.; Królikowska, M. Density and viscosity of binary mixtures of thiocyanate ionic liquids plus water as a function of temperature. J. Solut. Chem. 2012, 41, 1422–1445.
21. Liu, W.W.; Cheng, L.Y.; Zhang, Y.M.; Wang, H.P.; Yu, M.F. The physical properties of aqueous solution of room-temperature ionic liquids based on imidazolium: database and evaluation. J. Mol. Liq. 2008, 140, 68–72.
22. Lopes, J.N.C.; Gomes, M.F.C.; Husson, P.; Padua, A.A.H.; Rebelo, L.P.N.; Sarraute, S.; Tariq, M. Polarity, viscosity, and ionic conductivity of liquid mixtures containing [C_4C_1im][Ntf_2] and a molecular component. J. Phys. Chem. B 2011, 115, 6088–6099.
23. Danten, Y.; Cabaco, M.I.; Besnard, M. Interaction of water diluted in 1-butyl-3-methyl imidazolium ionic liquids by vibrational spectroscopy modeling. J. Mol. Liq. 2010, 153, 57–66.
24. Shekaari, H.; Mousavi, S.S.; Mansoori, Y. Thermophysical properties of ionic liquid, 1-pentyl-3-methylimidazolium chloride in water at different temperatures. Int. J. Thermophys. 2009, 30, 499–514.
25. Wojnarowska, Z.; Grzybowska, K.; Hawelek, L.; Święty-Pośpiech, A.; Masiewicz, E.; Paluch, M.; Sawicki, W.; Chmielewska, A.; Bujak, P.; Markowski, J. Molecular Dynamics and Glass Transition Behavior in Ionic Liquids. Mol. Pharm. 2012, 9, 1250–1261.
26. Sippel, P.; Dietrich, V.; Reuter, D.; Aumüller, M.; Lunkenheimer, P.; Loidl, A.; Krohns, S. Relaxation Dynamics in Ionic Liquids. J. Mol. Liq. 2016, 223, 635–642.
27. Bester-Rogac, M.; Stoppa, A.; Hunger, J.; Hefter, G.; Buchner, R. Electrical Conductivity and Permittivity of Ionic Liquids. Phys. Chem. Chem. Phys. 2011, 13, 17588–17598.
28. Mero, A.; Guglielmero, L.; D'Andrea, F.; Pomelli, C.S.; Guazzelli, L.; Koutsoumpos, S.; Tsonos, G.; Stavrakas, I.; Moutzouris, K.; Mezzetta, A. Thermophysical Characterization of Ionic Liquids. J. Mol. Liq. 2022, 354, 118850.

 doi:10.20944/preprints202603.0452.v1

29. Sturlaugson, A.L.; Fruchey, K.S.; Fayer, M.D. Orientational Dynamics of Room Temperature Ionic Liquid/Water Mixtures: Water-Induced Structure. J. Phys. Chem. B 2012, 116, 1777–1787.
30. Jacquemin, J.; Husson, P.; Padua, A.A.H.; Majer, V. Density and Viscosity of Several Pure and Water-Saturated Ionic Liquids. Green Chem. 2006, 8, 172–180.
31. Rodriguez, H.; Brennecke, J.F. Temperature and Composition Dependence of the Density and Viscosity of Binary Mixtures of Water Plus Ionic Liquid. J. Chem. Eng. Data 2006, 51, 2145–2155.
32. Huddleston, J.G.; Visser, A.E.; Reichert, W.M.; Willauer, H.D.; Broker, G.A.; Rogers, R.D. Characterization and Comparison of Hydrophilic and Hydrophobic Room Temperature Ionic Liquids Incorporating the Imidazolium Cation. Green Chem. 2001, 3, 156–164.
33. Thomaz, J.E.; Lawler, CM; Fayeret, MDl. The influence of water on the alkyl region structure in variable chain length imidazolium-based ionic liquid/water mixtures. J. Phys. Chem. B 2016, 120, 10350–10357.
34. Wuebbenhorst, M.; van Turnhout, J. Analysis of complex dielectric spectra. i. one-dimensional derivative techniques and three-dimensional modelling. J. Non-Cryst. Solids. 2002, 305, 40–49.
35. Johari, G.P.; Goldstein, M. Viscous liquids and the glass transition. II. Secondary relaxations in glasses of rigid molecules. J. Chem. Phys. 1970, 53, 2372–2388.
36. Kastner, S.; Köhler, M.; Goncharov, Y.; Lunkenheimer, P.; Loidl, A. High-frequency dynamics of type-B glass formers investigated by broadband dielectric spectroscopy. J. Non-Cryst. Solids. 2011, 357, 510–514.
37. Lunkenheimer, P.; Bobnar, V.; Pronin, A.V.; Ritus, A.I.; Volkov, A.A.; Loidl, A. Origin of apparent colossal dielectric constants. Phys. Rev. B. 2002, 66, 052105.
38. Havriliak S.; Negami S. A complex plane representation of dielectric and mechanical relaxation processes in some polymers. Polymer 1967, 8, 161–210.
39. Vogel, H. The temperature dependence law of the viscosity of fluids. Phys. Z. 1921, 22, 645–646.
40. Fulcher, G.S. Analysis of Recent Measurements of the Viscosity of Glasses. J. Am. Ceram. Soc. 1925, 8, 339–355.
41. Tammann, G; Hesse, W. Die Abhängigkeit der Viscosität von der Temperatur bie unterkühlten Flüssigkeiten. Z. Anorg. Allg. Chem. 1926, 156, 245–257.
42. Ito, N; Richert, R. Solvation dynamics and electric field relaxation in an imidazolium-PF6 ionic liquid: from room temperature to the glass transition. J. Phys. Chem. B. 2007, 111, 5016–5022.
43. Daguenet, C.; Dyson, J.P.; Krossing, I.; Oleinikova, A.; Slattery, J.; Wakai, C.; Weingaertner, H. Dielectric response of imidazolium-based room-temperature ionic liquids. J. Phys. Chem. B. 2006, 110, 12682–12688.
44. Nakamura, K.; Shikata, T. Systematic Dielectric and NMR Study of the Ionic Liquid 1-Alkyl-3-Methyl Imidazolium. ChemPhysChem. 2010, 11, 285–294.
45. Angell, C.A. Strong and fragile liquids, in: K.L. Ngai, G.B.Wright (Eds.), Relaxations in Complex Systems, NRL, Washington DC 1985, pp. 3–11.
46. Boehmer, R.; Ngai, K.L.; Angell, C.A.; Plazek, D.J. Nonexponential relaxations in strong and fragile glass formers. J. Chem. Phys. 1993, 99, 4201–4209.
47. Lunkenheimer P.; Loidl, A. Glassy Dynamics Beyond the α-Relaxation, in Broadband Dielectric Spectroscopy, F. Kremer and A. Schönhals, Eds., Berlin, Heidelberg: Springer, 2003, pp. 131–169.
48. C. Gainaru C.; Stacy, E.W.; Bocharova, V.; Gobet, M.; Holt, A.P.; Saito, T.; Greenbaum, S.; Sokolov, A.P. Mechanism of Conductivity Relaxation in Liquid and Polymeric Electrolytes: Direct Link between Conductivity and Diffusivity. J. Phys. Chem. B, 2016, 120, 11074–11083.
49. Mizuno, F.; Belieres, J.P.; Kuwata, N.; Pradel, A.; Ribes, A.; Angell, C.A. Highly decoupled ionic and protonic solid electrolyte systems, in relation to other relaxing systems and their energy landscapes, J. Non-Cryst. Solids 2006, 352, 5147–5155.
50. Sippel P.; Dietrich, V.; Reuter, D.; Aumüller, M.; Lunkenheimer, P.; Loidl, A.; Krohns, S. Impact of water on the charge transport of a glass-forming ionic liquid, Journal of Molecular Liquids. 2016, 223 635–642.
51. Ueno, K.; Zhao, T.; Watanabe, M.; Angell, C.A. Protic ionic liquids based on decahydroisoquinoline: lost superfragility and ionicity-fragility correlation, Phys. Chem. B. 2012, 116, 63–70.
52. Griffin, P.J.; Agapov, A.L.; Sokolov, A.P. Translation-rotation decoupling and nonexponentiality in room temperature ionic liquids. Phys. Rev. E. 2012, 86, 021508.

 doi:10.20944/preprints202603.0452.v1

53. Wojnarowska, Z.; Kołodziejczyk, K.; Paluch, K.J.; Tajber, L.; Grzybowska, K.; Ngai, K.L.; Paluch, M. Decoupling of conductivity relaxation from structural relaxation in protic ionic liquids and general properties. Phys. Chem. Chem. Phys. 2013, 15, 9205–9211.
54. Sippel, P.; Lunkenheimer, P.; Krohns, S.; Thoms, E.; Loidl, A. Importance of liquid fragility for energy applications of ionic liquids. Sci. Rep. 2015, 5, 13922.